Acta Pharmaceutica Sinica B 2019;9(2):421–432

Chinese Pharmaceutical Association
Institute of Materia Medica, Chinese Academy of Medical Sciences

Acta Pharmaceutica Sinica B

www.elsevier.com/locate/apsb
www.sciencedirect.com

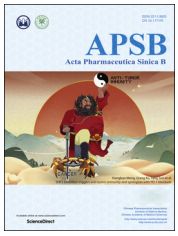

ORIGINAL ARTICLE

Redox-sensitive prodrug nanoassemblies based on linoleic acid-modified docetaxel to resist breast cancers

Meng Li[a], Liwen Zhao[a], Tao Zhang[a], Yue Shu[a], Zhonggui He[a], Yan Ma[c], Dan Liu[b,], Yongjun Wang[a,*]**

[a]*Wuya College of Innovation, Shenyang Pharmaceutical University, Shenyang 110016, China*
[b]*Key Laboratory of Structure-Based Drug Design and Discovery, Ministry of Education, Shenyang Pharmaceutical University, Shenyang 110016, China*
[c]*School of Chinese Materia Medica, Guangzhou University of Chinese Medicine, Guangzhou 510405, China*

Received 21 May 2018; received in revised form 12 July 2018; accepted 30 July 2018

KEY WORDS

Docetaxel;
Nanoassemblies;
Mono thioether bond;
Linoleic acid;
Pharmacokinetics;
Antitumor efficacy

Abstract Prodrug nanoassemblies, which can refrain from large excipients, achieve higher drug loading and control drug release, have been placed as the priority in drug delivery system. Reasoning that glutathione (GSH) and reactive oxygen species (ROS) are highly upgraded in tumor tissues which makes them attractive targets for drug delivery system, we designed and synthetized a novel prodrug which utilized mono thioether bond as a linker to bridge linoleic acid (LA) and docetaxel (DTX). This mono thioether-linked conjugates (DTX-S-LA) could self-assemble into nanoparticles without the aid of much excipients. The mono thioether endowed the nanoparticles redox sensitivity resulting in specific release at the tumor tissue. Our studies demonstrated that the nanoassemblies had uniform particle size, high stability and fast release behavior. DTX-S-LA nanoassemblies outperformed DTX solution in pharmacokinetic profiles for it had longer circulation time and higher area under curve (AUC). Compared with DTX solution, the redox dual-responsive nanoassemblies had comparable cytotoxic activity. Besides, the antitumor efficacy was evaluated in mice bearing 4T1 xenograft. It turned out this nanoassemblies could

Abbreviations: ALT, alanine transaminase; AST, aspartate transaminase; AUC, area under the curve; BUN, blood urea nitrogen; C-6, coumarin-6; CREA, creatinine; DDS, drug delivery system; DMSO, dimethyl sulfoxide; DSPE-PEG2K, 1,2-distearoyl-*sn*-glycero-3-phosphoethanolamine-*N*-[methoxy (polyethyleneglycol)-2000]; DTT, D,L-dithiothreitol; DTX, docetaxel; EDCI, *N*-(3-dimethylaminopropyl)-*N′*-ethyl carbodiimide hydrochloride; FBS, fetal bovine serum; GSH, glutathione; H_2O_2, hydrogen peroxide; HOBt, 1-hydroxybenzotriazole monohydrate; HPLC, high-performance liquid chromatography; IC_{50}, half maximal inhibitory concentration; LA, linoleic acid; MTT, 3-(4,5-dimethyl-2-thiazolyl)-2,5-diphenyl-2*H*-tetrazolium bromide; PBS, phosphate buffer saline; PDI, polydispersity index; PTX, paclitaxel; ROS, reactive oxygen species; SD, standard deviation; TLC, thin layer chromatography

*Corresponding author. Tel./fax: +86 24 23986325.
**Corresponding author. Tel./fax: +86 24 43520218.
E-mail addresses: sammyld@163.com (Dan Liu), wangyongjun@syphu.edu.cn (Yongjun Wang).

Peer review under responsibility of Institute of Materia Medica, Chinese Academy of Medical Sciences and Chinese Pharmaceutical Association.

https://doi.org/10.1016/j.apsb.2018.08.008

enhance anticancer efficacy by increasing the dose because of higher tolerance. Overall, these results indicated that the redox sensitivity nanoassemblies may have a great potential to cancer therapy.

1. Introduction

Docetaxel (DTX) is a kind of antineoplastic taxanes with wide antitumor spectrum, which is widely used in the treatment of breast cancer, lung cancer, gastric cancer and ovarian cancer[1]. The mechanism of DTX is to enhance the polymerization of microtubule and inhibit depolymerization, which results in the formation of stable nonfunctional microtubules, thereby hampering the mitosis of tumor cells[2,3].

Taxotere®, the commercial formulation of DTX with Tween 80 and 13% (*w*/*w*, ethanol/water) solution of ethanol as solvents, has been widely applied in clinical but accompanies with many side effects, such as nausea, alopecia, neutropenia, febrile neutropenia, and hypersensitivity reactions, which cause significant threats to patient health[4–7]. Thus, more extensive clinical use is delayed due to the lack of appropriate deliver vehicles. Nanoparticles as drug cargos show significant advantages in contrast with free drugs and play a crucial role in drug delivery system (DDS). The major advantages for nanoparticles over free drugs are that the nanoparticles can prolong the circulation time of drugs in the blood, achieve the passive targeting of drugs at the tumor site, achieve the effective uptake of drugs by tumor cells and regulate the release of drugs[8–10].

However, the traditional carrier-based nanoparticles also have drawbacks, such as the use of a large amount of excipients, low drug loading efficiency and crystallization[11,12]. In response to these disadvantages, intense interest has been rose in self-assembled prodrug nanoparticles. Prodrug, generally refers to compound that has little or no activity *in vitro* but can be metabolized to parent drug *in vivo*[13]. The merits of prodrug are that it can enhance the stability and selectivity of targeted cells, eliminate the side effects and cover discomfort smells of drugs[14]. Prodrug self-assemble into nanoparticles can totally make full use of the advantages of nanoparticles and circumvent the disadvantages. In other words, self-assembled prodrug nanoparticles not only target to tumors but also can increase drug loading efficiency and avoid the large use of excipients[15,16]. Self-assembly technique was also a common approach to generate clinically relevant paclitaxel (PTX) nanoformulations[17].

Fatty acids as dietary fats have been widely utilized to modify nanoparticles due to its biodegradability and biosafety[18]. A series of oleic acid-modified prodrug nanoparticles had been studied. Luo et al.[19] utilized oleic acid to conjugate with paclitaxel (PTX) to assemble nanoparticles. It turned out the oleic acid can improve the stability of anticancer drugs and achieve nutrition-target drug deliver. But much less is studied about the effect of linoleic acid (LA). Compared with oleic acid, the LA can clearly reduce the risk of coronary artery disease and increase the amount of serum lipoprotein in blood[20]. Besides, LA and its isomer originated in vegetable oil and meat could inhibit the initiation of carcinogenesis and exert a positive effect against proliferation of cancer[21]. LA is also an excellent proliferation inhibitor in HT-29 cells and could resist MCF-7 cell growth indicating the capacity of resisting breast cancer[22]. Co-incubation of breast cancer with PTX and γ LA showed that γ LA enhanced up to 8-fold the growth inhibitory activity of PTX indicating the γ LA and PTX had an excellent synergistic effect[23]. When modified LA in the vehicle to deliver DTX, the conjugates could significantly down-regulated antiapoptotic proteins and up-regulated pro-apoptotic proteins which indicated that the combination therapy had an enhancing effect on the up-regulation of apoptosis signaling[24]. One of the most successful cases which utilized LA is the LA–PTX conjugates. This conjugate can self-assemble into nanoparticles and has a good anti-tumor activity *in vitro*[25]. But the major drawback of this conjugates is the low release rate and degree which resulted from the lack of sensitive bonds. Compared to normal cells, tumor cells simultaneously overproduce reactive oxygen species (ROS) and glutathione (GSH) which has stimulated many attentions[26]. Based on these characteristics, we designed and synthesized mono thioether bond-bridged LA prodrug of DTX, abbreviated as DTX-S-LA. The DTX-S-LA can make full use of the concentration difference of GSH and ROS between tumor and normal cells to achieve rapid and specific release[19].

According to previous research[27,28], it was the first time to design and synthesize DTX-S-LA, a new compound with oxidation and reduction sensitivity which had not been studied yet. The LA was conjugated with DTX smartly by mono thioether to self-assemble into nanoparticles. We highlighted mono thioether to control drug release thus reduce systemic toxicity which may be caused by Taxotere®. Our designs that avoid adding large amount of excipients especially Tween 80, therefore offer promising strategies for increasing the safety of a broad range of therapeutic drugs. Thus, we speculate the DTX-S-LA nanoassemblies can exert an excellent treatment effect and reduce toxicity. Therefore, the stabilities, DTX release, cytotoxicity, antitumor efficacy and pharmacokinetic of DTX-S-LA/DSPE$_{2K}$ NPs were evaluated.

2. Materials and methods

2.1. Materials

LA, glycol, thiodiglycolic anhydride, 1-hydroxybenzotriazole monohydrate (HOBt), *N*-(3-dimethylaminopropyl)-*N*′-ethylcarbodiimide hydrochloride (EDCI) and D,L-dithiothreitol (DTT) were purchased from Aladdin Industrial Corporation (Shanghai, China). DTX was purchased from NanJing Jingzhu bio-technology Co., Ltd. (Nanjing, China). 1,2-Distearoyl-*sn*-glycero-3-phosphoethanolamine-*N*-[methoxy(polyethyleneglycol)-2000] (DSPE-PEG$_{2K}$) was purchased from Shanghai Advanced Vehicle Technology Pharmaceutical Co., Ltd. (Shanghai, China). Coumarin-6 (C-6) and Hoechst were purchased from Sigma–Aldrich (St. Louis, MO, USA). 3-(4,5-Dimethyl-2-thiazolyl)-2,5-diphenyl-2*H*-tetrazolium bromide

(MTT), fetal bovine serum (FBS) and DiR were purchased from Dalian Meilun Biotechnology Co., Ltd. (Dalian, China).

2.2. Design and synthesis of DTX-S-LA

153.0 mL (2.46 mol) glycol and 1.7 g (9.87 mmol) *p*-toluene sulfonic acid were heated to 110 °C with stirring under nitrogen protection. Then 8.4 g (29.95 mmol) LA was added into the reaction bottle in drops. Thin layer chromatography (TLC) was used to monitor the reaction. After the reaction, the product was extracted with methylbenzene, washed by saturated $NaHCO_3$ solution to neutral and dried with anhydrous sodium sulfate. Then the sodium sulfate was removed by filter. Finally, the product was purified by column chromatography method (*n*-hexane: ethyl acetate = 32:1, *v/v*). The yield was 65.7%.

0.22 g (1.67 mmol) thiodiglycolic anhydride, 0.25 g (1.67 mmol) HOBt and 0.32 g (1.67 mmol) EDCI were dissolved in 15 mL dichloromethane in ice bath. Then 0.35 g (1.08 mmol) linoleic acid-2-hydroxyethyl ester was added dropwise to the solution with stirring for 30 min under nitrogen protection. Next, the reaction temperature was changed to 25 °C and stirring was sustained for 12 h. The reaction was monitored using TLC analysis. The dichloromethane solution was utilized to extract the product. The saturated NaCl solution was used to wash the product for three times. Then the product was dried by adding anhydrous sodium sulfate. At last, the product was filtered, dried and purified. The yield of objective product (2-((2-(2-(((9*E*,12*E*)-octadeca-9,12-dienoyl)oxy)ethoxy)-2-oxoethyl)thio)acetic acid) was 56.4%.

2.1 g (2.6 mmol) DTX, 0.5 g (2.6 mmol) EDCI, 0.35 g (2.6 mmol) HOBt and 1.4 g (3.1 mmol) 2-((2-(2-(((9*E*,12*E*)-octadeca-9,12-dienoyl)oxy)ethoxy)-2-oxoethyl)thio) acetic acid were dissolved in 50 mL dichloromethane. Then the temperature of the solution was declined to 0 °C and stirred for 30 min under nitrogen. After that, the reaction temperature was transferred to 25 °C to react for 24 h. TLC was applied to monitor the reaction. Then the product was processed using similar methods to previous step. Lastly, preparative liquid chromatograph was utilized to purified the final product. Eventually, a white solid, that is, target product (DTX-S-LA) was gained. The yield was 45.9%.

2.3. Preparation and characterization of DTX-S-LA/DSPE$_{2K}$ NPs

The nanoparticles were prepared by one step precipitation method. In short, 4 mg accurately weighed prodrug and 20% DSPE-PEG_{2K} (*w/w*) were added to 200 μL anhydrous ethanol, blended well, added dropwise into 2 mL deionized water with stirring (800 rpm, K-MSH-Pro-6A, JKI, Shanghai, China) at room temperature. Then anhydrous ethanol was removed by rotary vacuum distillation at 37 °C. Next, the solution was diluted with deionized water to 2 mL. Finally, centrifuging at 10,000 rpm (TGL-16B, Anting Scientific Instrument Factory, Shanghai, China) for 5 min to exclude the free drugs.

The particle size, zeta potential and polydispersity index (PDI) of prodrug nanoparticles were measured by a Zetasizer (Nano ZS, Malvern, UK) in triplicate. The morphology of the nanoparticles was characterized by transmission electron micrographs (TEM, Hatachi HT7700). Briefly, the nanoparticle solution was dripped to the copper grid for 30 s and dried. Then 1% phosphotungstic acid solution was dripped to the copper to stain the sample. After 1–2 min, the solution was blotted up and dried. This sample was observed by TEM.

2.4. Physical stability

In order to evaluate the stability of nanoparticles, 1 mL DTX-S-LA/DSPE$_{2K}$ NPs (2 mg/mL) was incubated in 9 mL PBS (pH 7.4) containing 10% FBS at 37 °C for 48 h. Besides, nanoparticle preparation (0.5 mg/mL) was stored at 4 °C up to 3 months to assess the long-term stability. The particle size and PDI were measured at pre-determined intervals.

2.5. In vitro drug release

The drug release study was performed by dialysis method. To confirm the oxidation sensitivity, 0, 5, and 10 mmol/L hydrogen peroxide (H_2O_2) was respectively added into phosphate buffer saline (PBS, pH 7.4) containing 30% ethanol to be as release media[19,29]. Then 200 μL nanoparticles was placed in dialysis bags and soaked in conical flasks which were placed in air bath (CHA-S, Guohua Electric Applance Co., Ltd., Jiangsu, China) with shaking (100 rpm) at 37 °C. Sampling 0.2 mL and replenishing equal volume of release media after 2, 4, 6, 8, 10, 12 and 24 h. The quantitative analysis was carried out by high-performance liquid chromatography (HPLC) on a reverse ODS Cosmosil-C18 column (150 mm × 4.6 mm, 5 μm). The composition of mobile phase was acetonitrile/water (55:45, *v/v*) and the flow rate was 1.0 mL/min. The H_2O_2 was replaced with DTT to measure the reduction sensitivity using the same method as above.

2.6. Cytotoxicity assay

The *in vitro* anticancer activity was investigated by MTT assay. Briefly, a certain density of 4T1 cells (1×10^3) were seeded in 96-well plates and cultivated in a humidified atmosphere with 5% CO_2 at 37 °C for 12 h. Then, the culture medium was replaced by 200 μL fresh medium which containing DTX solution and DTX-S-LA/DSPE$_{2K}$ NPs, respectively. The plates were incubated for 48 and 72 h. Then, 10 μL MTT solution was added to each well containing cells. After cultivating for 4 h, the solution was removed completely and 200 μL dimethyl sulfoxide (DMSO) was added to each well. Next, the plates were vibrated for 10 min on the mini shaker to dissolve the formazan. The absorbance value of each hole in 96 well plates was measured at 490 nm by a multi-function enzyme scale (Model500, USA). The inhibition rate was calculated by the following equation, inhibition rate (%) = $(1\text{-}A_{sample}/A_{control}) \times 100$. The half maximal inhibitory concentration (IC_{50}) was gained by nonlinear regression analysis.

2.7. Cellular uptake

The 4T1 cells were seeded in 24 well plates at a density of 1×10^5 cells/well for 24 h. C-6-labeled DTX-S-LA/DSPE$_{2K}$ NPs were prepared by one step precipitation method. Briefly, the prodrug, DSPE-PEG_{2K} and C-6 were dissolved in ethanol and added dropwise to water with stirring. Under these conditions, the self-assembly of C-6-labeled DTX-S-LA/DSPE$_{2K}$ NPs occurred spontaneously. Then the medium was replaced by free C-6 solution and C-6-labeled DTX-S-LA/DSPE$_{2K}$ NPs with the

equivalent concentration of C-6 (250 ng/mL) and incubated for 0.5, 1, 2 and 4 h. After incubation, the cells were rinsed thrice with cold PBS and fixed by 4% formaldehyde. Hoechst was used as the coloring matter for cell nucleus. Finally, the samples were observed *via* confocal laser scanning microscopy (Zeiss LSM 510 Meta, Germany).

For quantitative determination, 4T1 cells were seeded in 24-well plates at a certain density (1×10^5) and cultured for 24 h. Then free C-6 solution and C-6-labeled DTX-S-LA/$DSPE_{2K}$ NPs with the equivalent C-6 (250 ng/mL) were added to each wall respectively. Incubation for 0.5, 1, 2 and 4 h. After that, the cells were collected, centrifugated, filtered and analyzed by BD FACSVerse flow cytometer.

2.8. *Animal studies*

All the animals were provided by the Laboratory Animal Center of Shenyang Pharmaceutical University and all the animal experiments in this work abided by the Guide for Care and Use of Laboratory Animals approved by the Institutional Animal Ethical Care Committee (IAEC) of Shenyang Pharmaceutical University (Shenyang, China).

2.9. *Biodistribution study*

BALB/c-tumor-bearing mice were utilized to evaluate the biodistribution of prodrug nanoparticles. DiR-labeled DTX-S-LA/$DSPE_{2K}$ NPs were prepared by referring to the preparation method of C-6-labeled DTX-S-LA/$DSPE_{2K}$ NPs Free DiR solution and DiR labeled DTX-S-LA/$DSPE_{2K}$ NPs with equivalent DiR (2 mg/kg) were administrated *via* tail vein. After post injection for 6 and 24 h, the fluorescence intensity was measured by *in vivo* imaging system (IVIS) spectrum small-animal imaging system.

2.10. *Pharmacokinetics study*

The SD rats were randomly divided into two groups ($n = 5$) to determine the pharmacokinetics of DTX solution and prodrug nanoparticles. Briefly, DTX solution and DTX-S-LA/$DSPE_{2K}$ NPs with equivalent DTX (5 mg/kg) were administrated *via* tail vein, and 400 µL blood were collected from the orbit at predetermined time intervals. Then the supernatant was collected after centrifugation. Acetonitrile was used for the precipitation of protein. The samples were analyzed by HPLC–MS/MS. C18 column (100 mm × 2.1 mm, 5 µm) was utilized and the flow rate was 0.2 mL/min. To determine the concentration of DTX-S-LA, the mobile phase was acetonitrile/water (95:5, *v/v*), and DTX was determined with a gradient elution: 0–0.5 min, 70% water; 0.51–2.5 min, 5% water; 2.6–3.0 min, 70% water.

2.11. *In vivo antitumor efficacy*

The BALB/c female mice weighed 18–22 g were fed for one week to adapt to the environment. Then the cultured 4T1 cells (5×10^6) were subcutaneously to the right axilla of mice. The mice were divided into 4 groups ($n = 5$) which were administered intravenously every two days with saline (control), DTX solution (10 mg/kg), low dose DTX-S-LA/$DSPE_{2K}$ NPs (10 mg/kg) and high dose DTX-S-LA/$DSPE_{2K}$ NPs (30 mg/kg), respectively. The volume of tumor and the body weight were measured every two days. After 8 days, 0.2 mL serum were gained to examine the hepatorenal function including blood urea nitrogen (BUN), creatinine (CREA), aspartate transaminase (AST), alanine transaminase (ALT). Then the mice were sacrificed, and the major organs (heart, liver, spleen, lung, and kidney) and the tumors were dissected for hematoxylin and eosin (H & E).

2.12. *Statistical analysis*

The results were expressed as mean ± standard deviation (SD). Statistical significances were determined using the Student's *t*-test. A *P*-value < 0.05 was considered to be significant, and a *P*-value < 0.01 was considered as highly significant.

3. Results

3.1. *Design and synthesis of DTX-S-LA*

A DTX prodrug contained mono thioether bond which was sensitive to oxidation–reduction was synthesized (Scheme 1). The compound structure was confirmed by ^{1}H NMR (Fig. 1A) and MS (Fig. 1B).

3.2. *Preparation and characterization of DTX-S-LA/$DSPE_{2K}$ NPs*

The schematic representation was shown in Scheme 2. Compared with traditional nanoparticles, the DTX-S-LA/$DSPE_{2K}$ NPs had high drug loading (53.4%) and encapsulation efficiency (98.8%). The mean diameter of the nanoparticles was about 100 nm (Fig. 2B), and the zeta potential is − 21.5 mV. TEM showed the morphology of the nanoparticle was a round sphere (Fig. 2C).

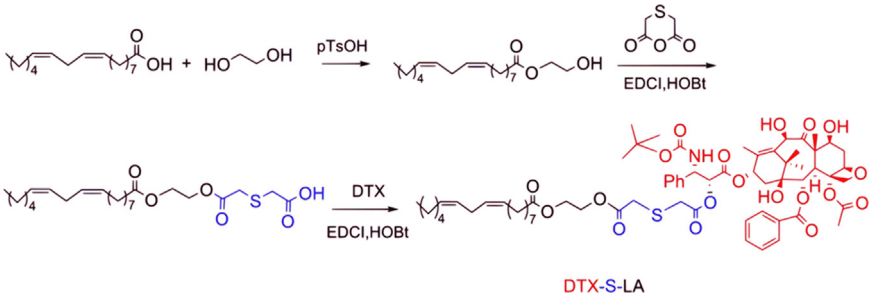

Scheme 1 The synthetic route of DTX-S-LA.

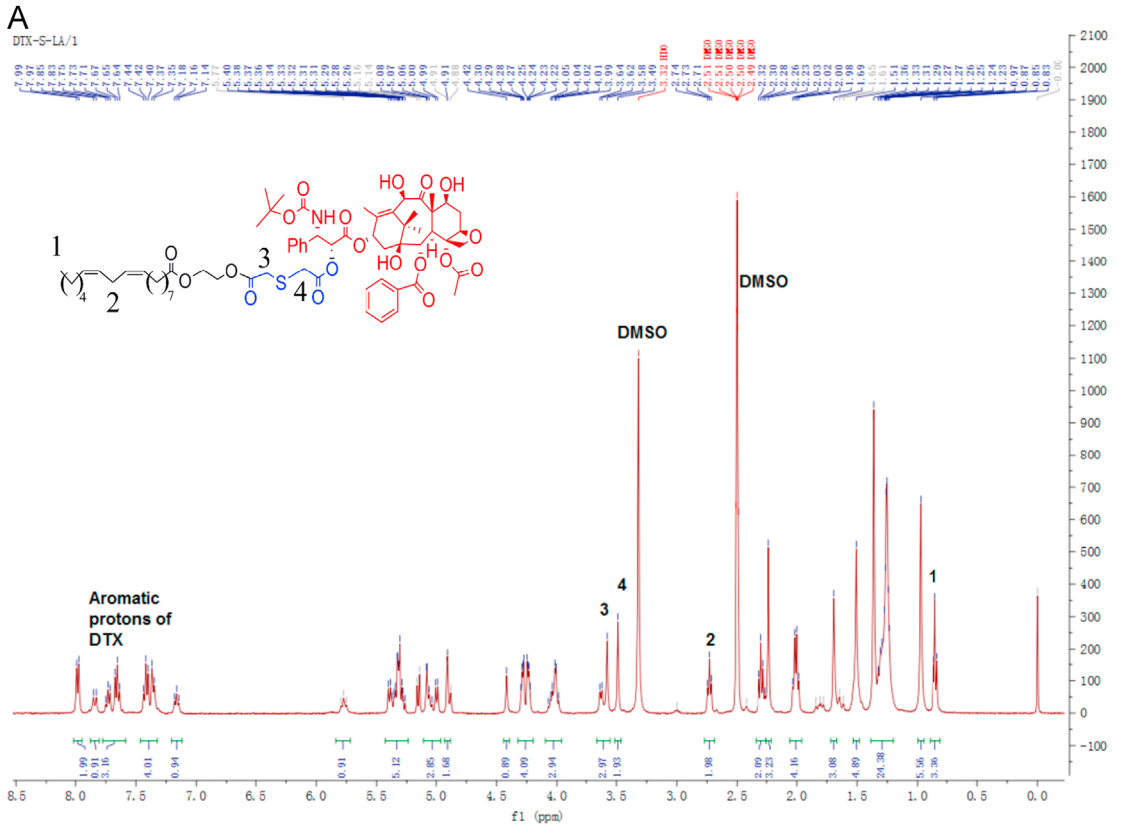

Figure 1 (A) The ^{1}H NMR spectra of DTX-S-LA. (B) The MS spectra of DTX-S-LA.

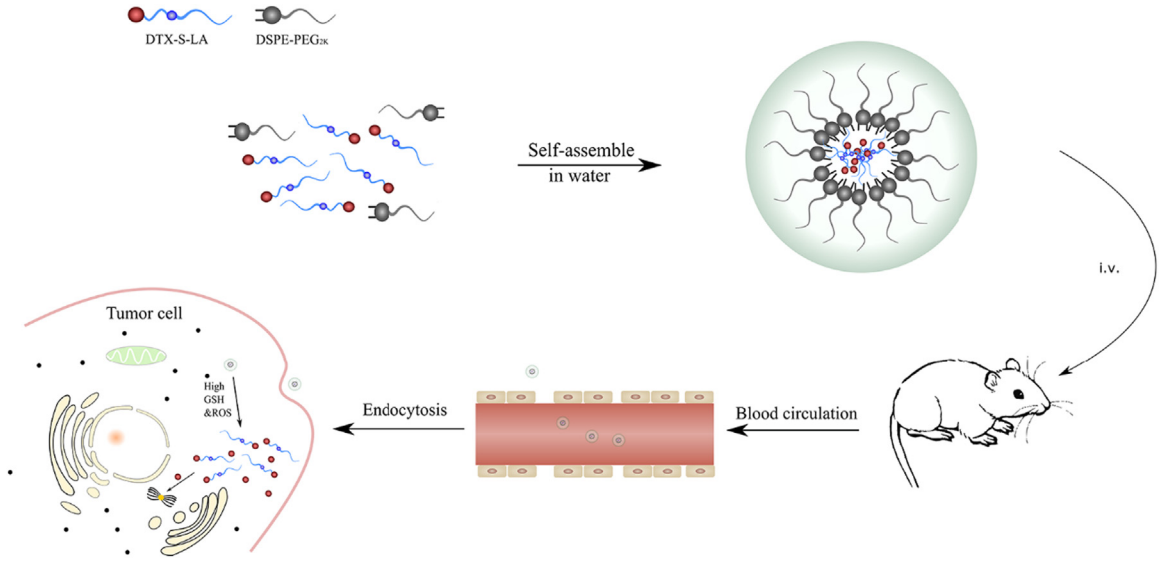

Scheme 2 Schematic representation of DTX-S-LA/DSPE$_{2K}$ NPs.

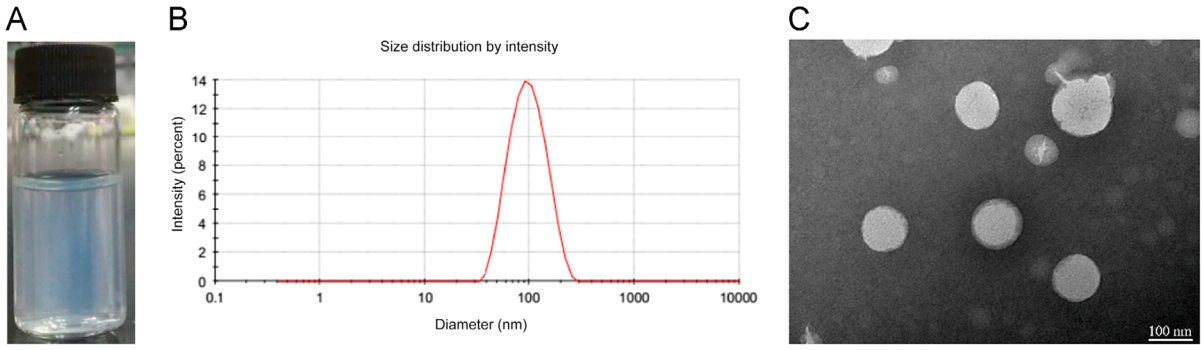

Figure 2 (A) Appearance of nanoassemblies with light blue opalescence. (B) The size distribution of nanoparticles. (C) Morphology of DTX-S-LA/DSPE$_{2K}$ NPs by TEM.

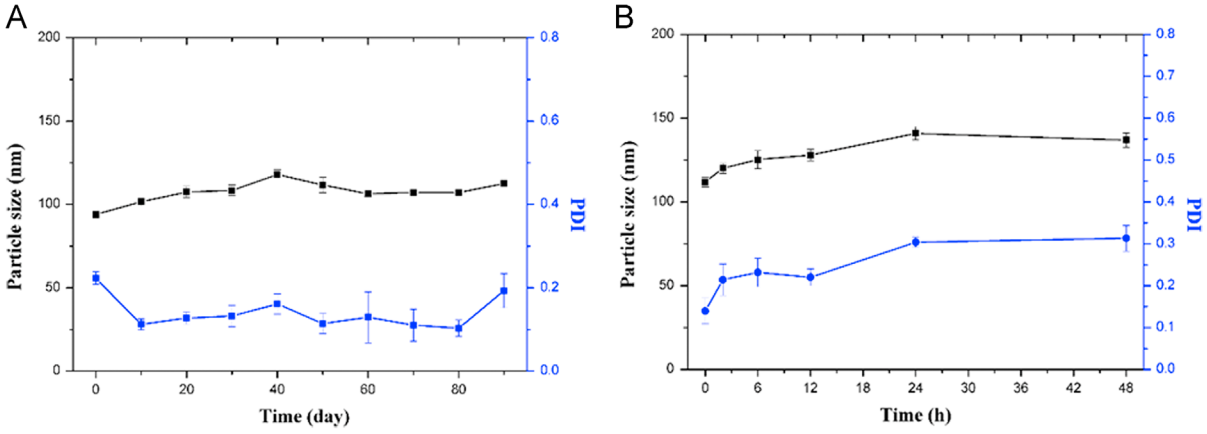

Figure 3 (A) The long-term stability of DTX-S-LA/DSPE$_{2K}$ NPs at 4 °C. (B) The particle size and PDI of DTX-S-LA/DSPE$_{2K}$ NPs in the PBS containing 10% FBS.

3.3. *Physical stability*

The physical stability of prodrug nanoparticles was investigated. According to the Fig. 3A, the particle size remained 100 ± 10 nm and the PDI was always between 0.1–0.2 in three months when the preparation was placed in 4 °C. In addition, the particle size of nanoparticles in the PBS containing 10% FBS had no obvious change (Fig. 3B). From the data, it could draw the conclusion that the DTX-S-LA/DSPE$_{2K}$ NPs had excellent physical stability.

3.4. *In vitro drug release*

In the drug release experiment, 30% ethanol–PBS was chosen as the release media. As shown in the Fig. 4, less than 38% DTX was released in the release media containing no H_2O_2 or DTT. By contrast, 82% and 60% DTX were released in the presence of 10 mmol/L and 5 mmol/L H_2O_2, respectively, which indicated DTX-S-LA/DSPE$_{2K}$ NPs had excellent oxidation sensitivity. Besides, 50% DTX was released in 10 mmol/L DTT. Also, higher than the group containing no DTT, suggesting DTX-S-LA/DSPE$_{2K}$ NPs had reduction sensitivity.

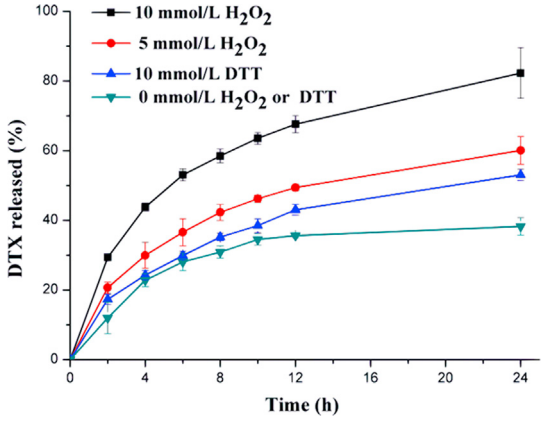

Figure 4 Drug release from DTX-S-LA/DSPE$_{2K}$ NPs in the presence of DTT or H_2O_2 ($n = 3$).

3.5. *Cytotoxicity assay*

The cell viability was assessed by MTT method to determine the cytotoxic activity of DTX solution and DTX-S-LA/DSPE$_{2K}$ NPs As

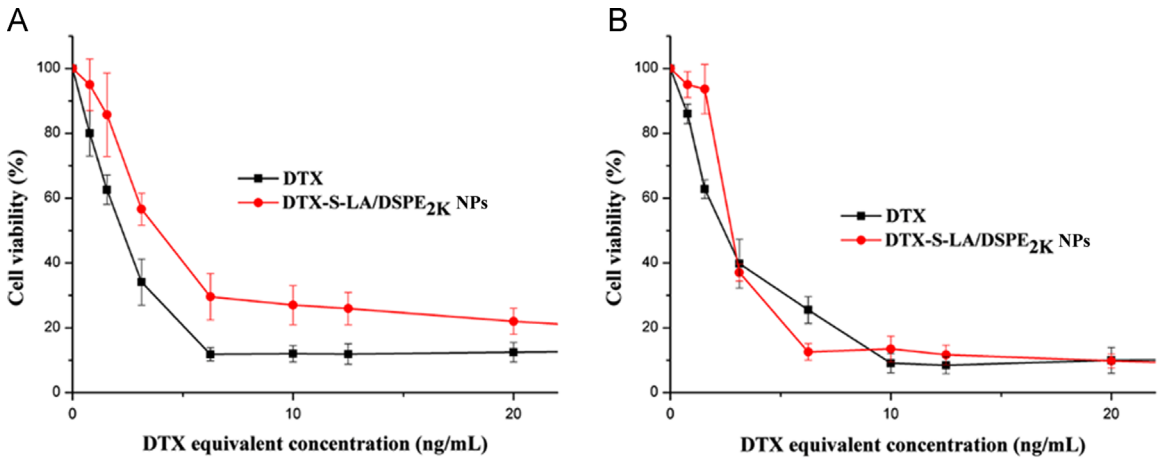

Figure 5 Anticancer activity of various concentrations of DTX and DTX-S-LA/$DSPE_{2K}$ NPs *in vitro* for 48 h (A) and 72 h (B).

shown in Fig. 5A, the value of cell viability treated with DTX solution was slightly lower than that treated with DTX-S-LA/$DSPE_{2K}$ NPs at 48 h. But the two groups' cell viability became nearly the same at 72 h (Fig. 5B). Comparing two graphs, it was obvious that the inhibition of tumor cells depended on the release rate of parent drugs. Consequently, the cytotoxicity of the prodrug self-assembled nanoparticles *in vitro* was lower than DTX solution for it needed more time to release parent drug. The IC_{50} values of DTX solution and DTX-S-LA/$DSPE_{2K}$ NPs at 48 h were 2.28 and 4.02 μg/mL, respectively.

3.6. *Cellular uptake*

The 4T1 cells were utilized to perform the cellular uptake study. As shown in Figs. 6 and 7, the DTX-S-LA/$DSPE_{2K}$ NPs always exhibited much stronger intracellular fluorescence intensity than free C-6 group, indicating that the prodrug nanoparticles had better cellular uptake efficiency than that of free solution. Besides, the intracellular fluorescence intensity enhanced with time which meant the cellular uptake was time dependent.

3.7. *Biodistribution study*

Biodistribution of prodrug nanoassemblies was performed in 4T1-bearing mice. As shown in Fig. 8, the DiR solution mainly accumulated in spleen and lung. By contrast, very strong fluorescence intensity could be observed in the tumor for the group of DTX-S-LA/$DSPE_{2K}$ NPs. And the fluorescent signals in tumors increased over time from 6 to 24 h which meant the

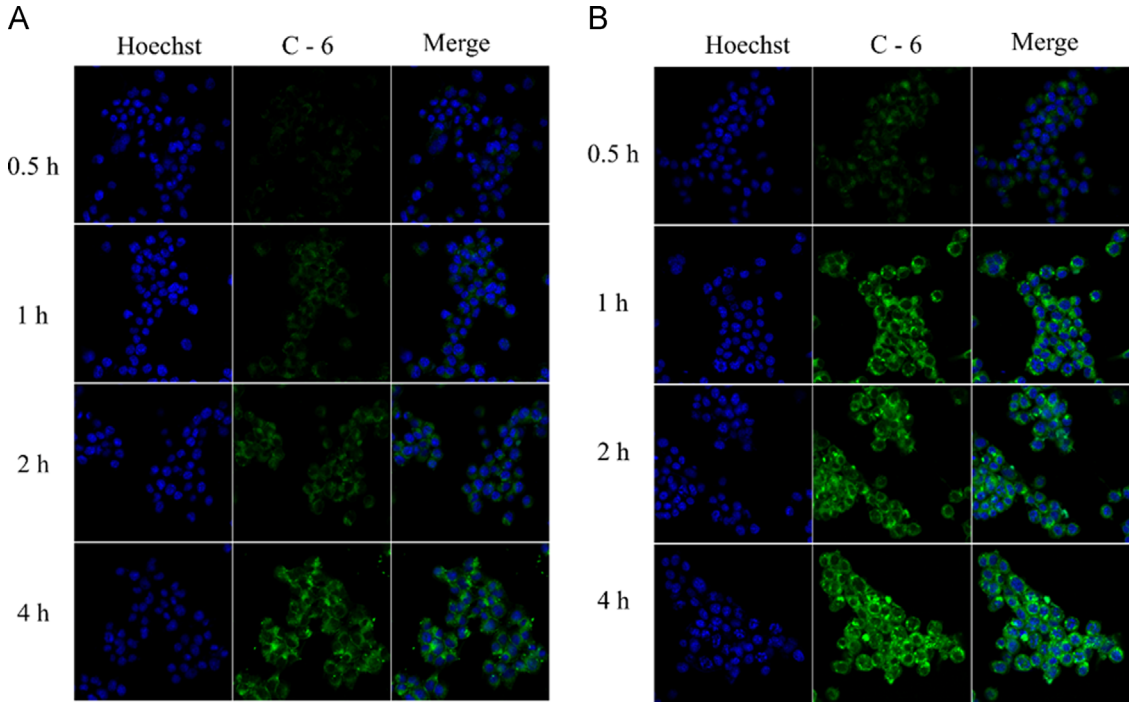

Figure 6 Confocal laser scanning microscopy images of 4T1 cells incubated with free coumarin-6 (A) or coumarin-6-labeled prodrug nanoassemblies (B).

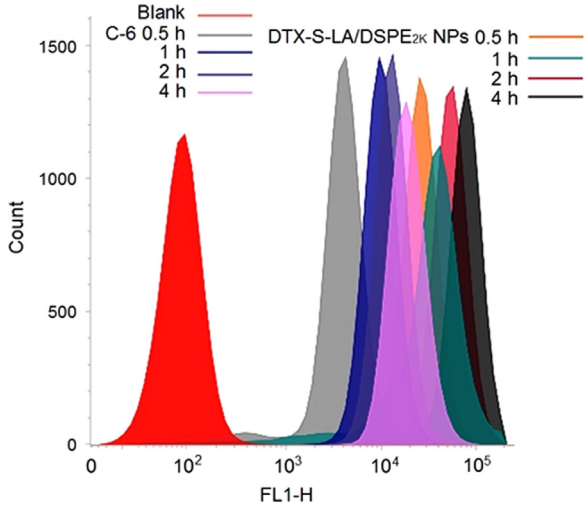

Figure 7 Cellular uptake in 4T1 cells after incubation by flow cytometry.

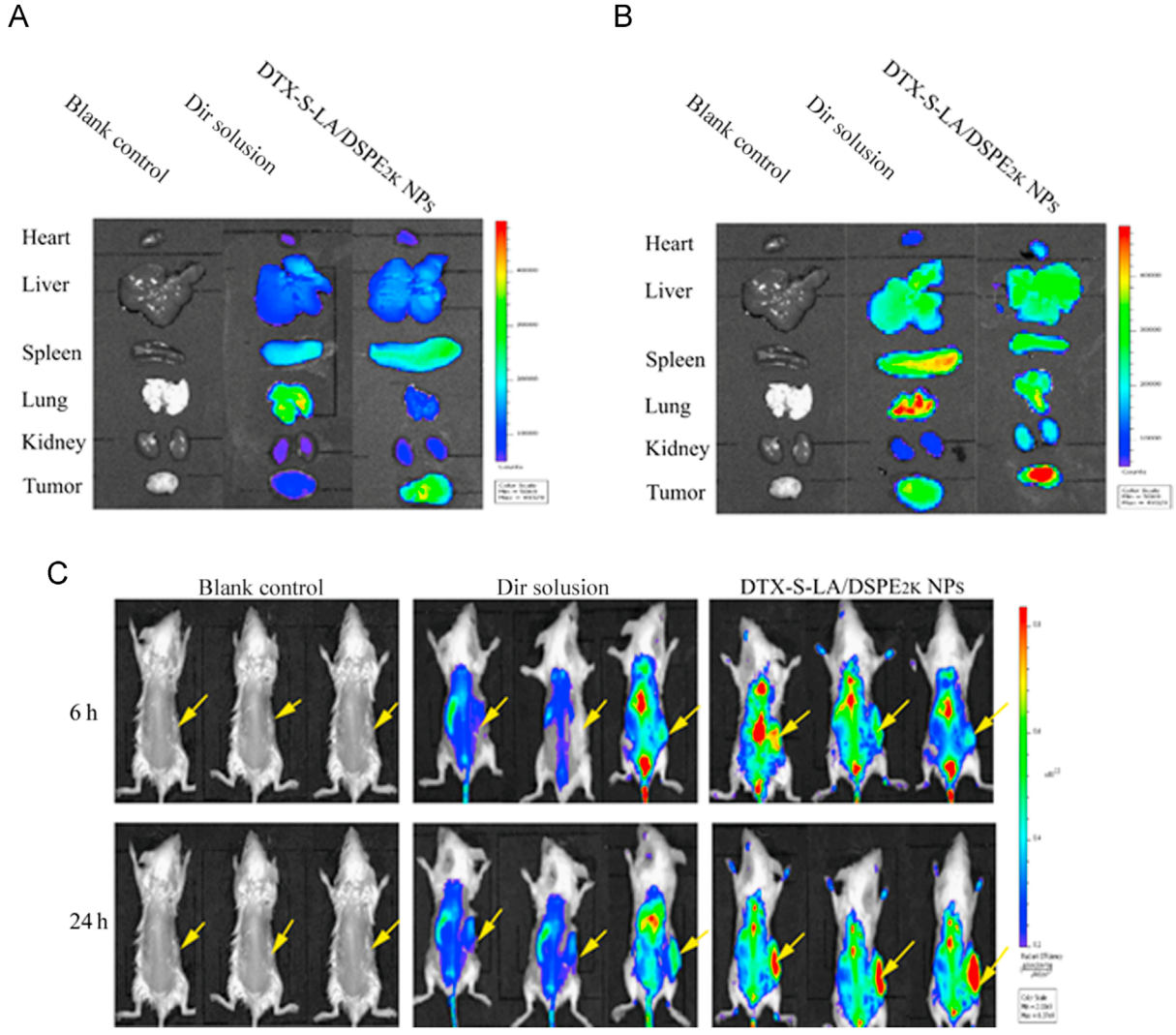

Figure 8 *Ex vivo* biodistribution of DiR solution and DiR-labeled prodrug nanoassemblies at 6 h (A) or 24 h (B). (C) The tumor (indicated by arrows) bearing mice were imaged after injection of DiR solution and DiR-labeled prodrug nanoassemblies.

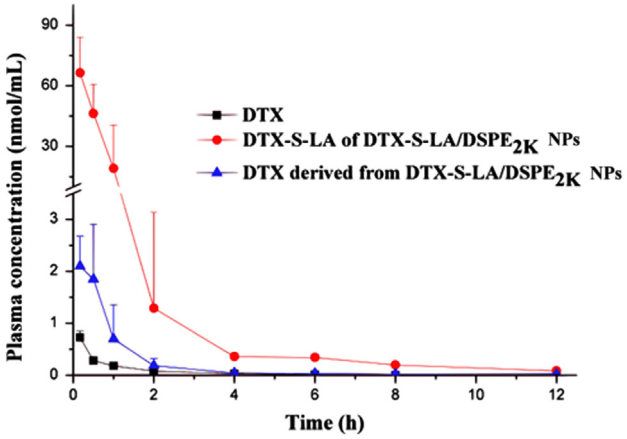

Figure 9 Drug concentration-time curve of DTX solution, DTX-S-LA and DTX derived from prodrug nanoparticles after tail vein injection ($n = 5$).

accumulation in tumor was time depended. These results suggested that the extended cycle time could promote the accumulation of nanoparticles in the tumor by EPR effect.

3.8. *Pharmacokinetics study*

The pharmacokinetics evaluation was performed using drug concentration-time curve. As shown in Fig. 9, the DTX-S-LA/$DSPE_{2K}$ NPs can significantly increase the area under the curve (AUC) and $t_{1/2}$, which indicated the prodrug nanoparticles can prolong circulation time so that the nanoparticles could be delivered to the tumor site through the EPR effect and the antitumor effect could be largely enhanced. The major pharmacokinetic parameters were listed in Table 1. In fact, the AUC and $t_{1/2}$ of nanoparticles was 93 times and 1.3 times of that for DTX injection, respectively.

3.9. *In vivo antitumor efficacy*

BALB/c female mice were utilized to evaluate antitumor efficacy *in vivo*. As shown in the Fig. 10A, the dramatic distinctions of four groups' tumor volumes were seen in the last four days. The tumor volume of mice treated with saline increased exponentially to 465 mm^3 in the eighth day. Compared with DTX solution, slower tumor growth was achieved by administering intravenously with high dose DTX-S-LA/$DSPE_{2K}$ NPs.

According to the Fig. 10B, the body weight of mice administered with DTX solution declined significantly. In contrast, the mice treated with DTX-S-LA/$DSPE_{2K}$ NPs showed steady body weight and better health. One particularly remarkable fact highlighted by the figure was that the high dose (30 mg/kg) of DTX-S-LA/$DSPE_{2K}$ NPs was as safe as low dose, which hinted the prodrug nanoparticle preparation had higher tolerance dose. The values of tumor burden (tumor burden = tumor weight / body weight × 100%) were given in Fig. 10C.

As shown in the Fig. 10D, no difference was discovered between hematological parameters of mice treated with saline and DTX-S-LA/$DSPE_{2K}$ NPs. However, the DTX solution-treated mice's hematological parameters were abnormal and had significant difference compared with mice treated with saline, especially the value of ALT was two times higher than that of saline group. The result indicated that the DTX solution had higher hepatotoxicity.

The tumor image was shown in Fig. 11A. As shown in H & E result (Fig. 11B), the tumor sections of DTX treated mice just had little fibrosis. But large necrotic areas could be seen in the tumor sections of DTX-S-LA/$DSPE_{2K}$ NPs treated group. Furthermore, different levels of liver metastasis could be found in liver sections of DTX treated groups which could be hardly found in sections of DTX-S-LA/$DSPE_{2K}$ NPs treated group.

4. Discussion

Unlike other DTX–fatty acid conjugates, we utilized mono thioether to bridge LA and DTX which was rarely studied. The hydrophobic conjugates could self-assemble into NPs alone in deionized water without any surfactant. The particle size could remain stable within three months in 4 °C (Supporting Information Fig. S1), indicating good stability of non-PEGylated nanoassemblies. DSPE-PEG_{2K} was used to improve the colloidal stability. The self-assembly mechanism of the hydrophobic prodrugs was not completely clear yet. Multiple mechanisms were found to be involved in the self-assembly process, including inhibition of crystallization, structural flexibility (LA) and intermolecular π–π stacking (DTX)[14,19]. A total of 10% ethanol was utilized in the preparation process. A small amount of ethanol might still remain

Table 1 The major pharmacokinetic parameters of DTX solution and DTX-S-LA/$DSPE_{2K}$ NPs.

Formulations	Determined	C_{max} (nmol/mL)	T_{max} (h)	AUC_{0-24} (nmol h/mL)	$t_{1/2}$ (h)
DTX solution	DTX	0.7 ± 0.1	0.17 ± 0.0	0.7 ± 0.1	3.1 ± 1.3
DTX-S-LA/$DSPE_{2K}$ NPs	DTX	1.5 ± 0.7	0.3 ± 0.2	2.8 ± 0.95	3.2 ± 0.9
	DTX-S-LA	66.6 ± 19.7	0.2 ± 0.15	65.5 ± 27.7	4.0 ± 1.5

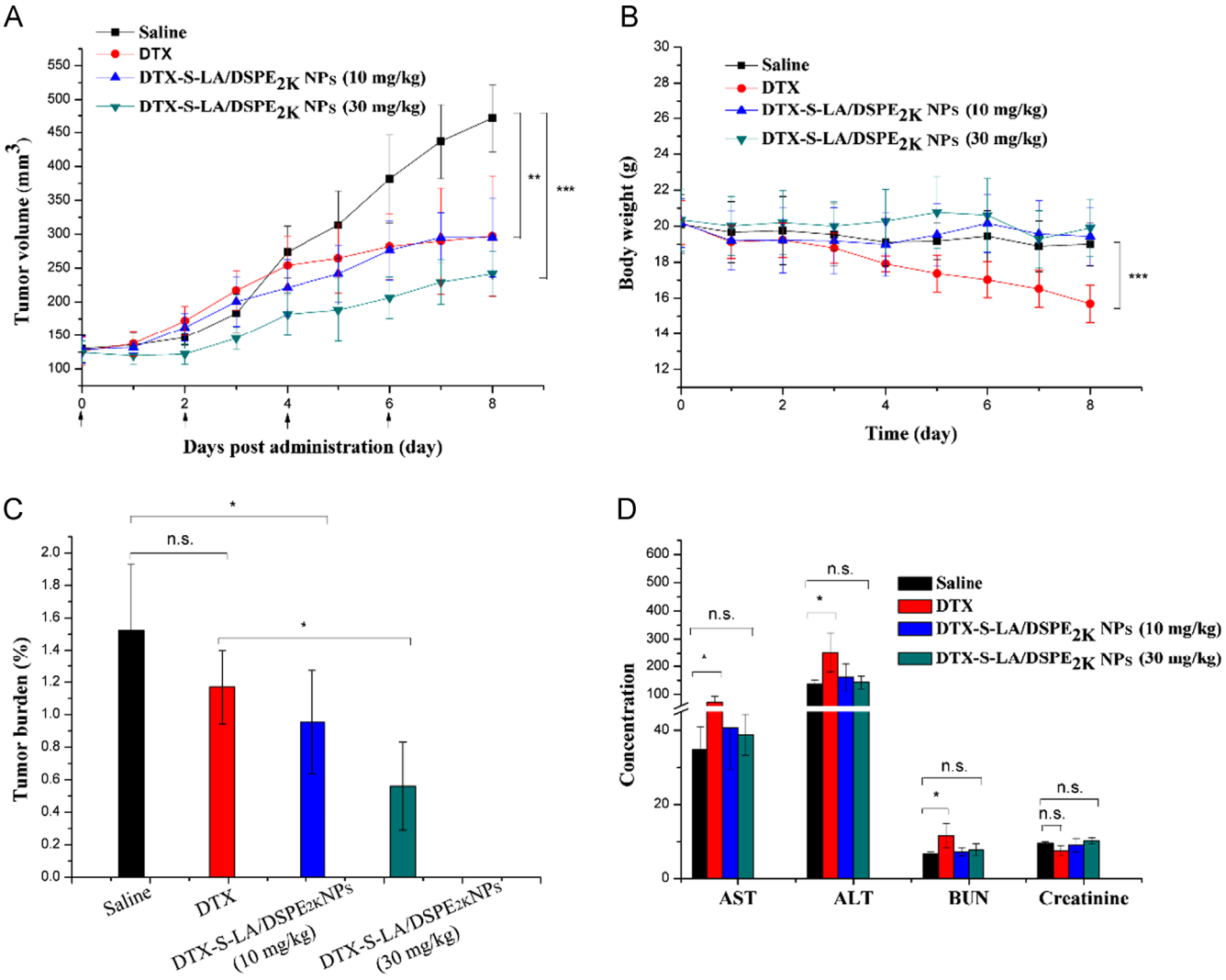

Figure 10 The changes of tumor volume (A) and body weight (B) of mice after various treatments ($n = 5$). (C) Tumor burden after the last treatment. (D) Study on hepatotoxicity induced by different preparations (the unit for AST, ALT, BUN and Creatinine is U/L, U/L, mmol/L and μmol/L, respectively).

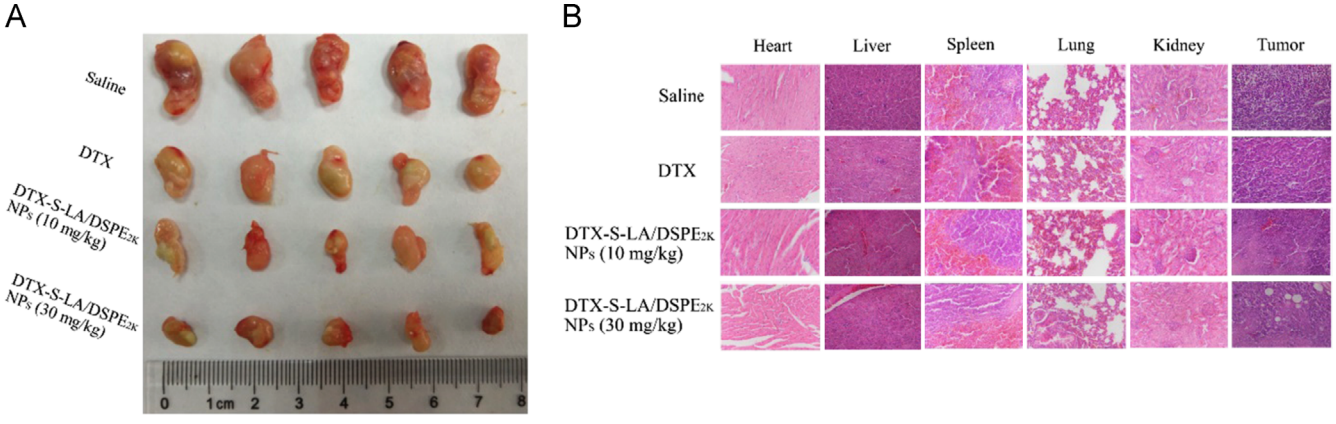

Figure 11 (A) The image of tumors after last treatment. (B) The H & E of major organs and tumors after last treatment.

after rotary vacuum distillation. The detailed effect of residual ethanol on drug action was still unclear now. From Fig. 3, the NPs could remain stable both in 4 °C and FBS medium, indicating the residual alcohol was too minute to influence the stability of NPs. Wang et al.[30] prepared the NPs with a final ethanol concentration of 2%–5% also showed good stability.

The key to DTX-S-LA responsive to both GSH and ROS leading to fast release of DTX was the mono thioethers that can utilize the two opposite stimuli. DTX-S-LA was a hydrophobic conjugate. The ester bond conjugated with DTX was very sensitive to its hydrophilicity/hydrophobicity environment and electron-withdrawing effect. The mono thioether located in the α-position of the ester and thus would greatly influence the environment of the ester bond. Once the mono thioether oxidized to sulfone or sulphone which were electron-withdrawing and hydrophilic, would promote the hydrolysis of neighboring ester bonds to release DTX. Besides, when the nanoassemblies endocytosed into cells, the thiolysis process which initiated by the thiol group of GSH would facilitate the DTX release from prodrugs[19,29]. The release study *in vitro* indicated that drug release of mono thioether-based hydrophobic conjugates could be triggered by GSH and ROS. ROS in tumor was hard to be quantified accurately for it consists of many types including the superoxide anion (O^{2-}), hydrogen peroxide (H_2O_2), and hydroxyl radicals ($\cdot OH$), and one of the ROS species can convert into another through a series of reaction processes. The determined concentration of H_2O_2 was to testify the oxidation sensitivity of nanoassemblies was concentration dependence. The nanoparticles released 82% and 50% DTX in 10 mmol/L H_2O_2 and DTT, respectively, suggesting DTX-S-LA was more likely to be oxidized, thus the release rate and degree mainly depended on the concentration of ROS. Rapid release of active DTX within tumor cells would facilitate the drug-induced apoptosis of tumor cells. Longer time was needed to release DTX from DTX-S-LA/$DSPE_{2K}$ NPs because of the slow cleavage of the mono thioether bond, thus the cytotoxicity of DTX-S-LA/$DSPE_{2K}$ NPs was slightly weaker than that of DTX solution at 48 h. In addition, the parent drug release was dose- and time-dependent leading to stronger cytotoxicity of DTX-S-LA/$DSPE_{2K}$ NPs at 72 h than that of 48 h.

Various enzymes including GSH existed in rat plasma causing slightly release of DTX from DTX-S-LA/$DSPE_{2K}$ NPs. Thus, both DTX-S-LA and DTX derived from prodrugs were measured in pharmacokinetic study. And either of AUC and $t_{1/2}$ was significantly extended when compared with DTX solution. The C_{max} (nmol/mL) of derived DTX and DTX-S-LA/$DSPE_{2K}$ NPs was 1.5 ± 0.7 and 66.6 ± 19.7, respectively. And the AUC of DTX-S-LA/$DSPE_{2K}$ NPs was 21 times more, which turned out only a small proportion of prodrug degraded in the blood circulation. The degradation was slow but DTX get eliminated very fast, thus the derived DTX achieved the peak value with no derivation time. Prodrug nanoassemblies indeed displayed prolonged retention, slow prodrug activation and free drug release in the circulation.

The AUC of DTX derived from prodrug NPs was higher than DTX solution. However, the group of DTX solution instead of prodrug NPs was revealed the poor bio-tolerance. The incidence of toxicity and adverse effects was related to the tissue distribution of drugs which could be partly influenced by the preparation and surfactant vehicles[31]. Hence, the DTX derived from prodrug NPs and DTX solution may possess different disposition profiles. The DTX solution caused more severe hepatotoxicity (Fig. 10) which hinted the DTX might mainly accumulate in liver and kidney. Besides, numerous adverse effects related to Taxotere® formulation vehicles have been described, including acute hypersensitivity reactions and peripheral neuropathies[32]. The amount of surfactant vehicles which comprised the standard solvent system for docetaxel solution (DTX:Tween 80 = 1:16, molar ratio) was far higher than the amount of excipient used in NPs (DTX-S-LA:DSPE-PEG_{2K} = 1:0.087, molar ratio). Although DTX-S-LA/$DSPE_{2K}$ NPs (10 mg/kg) demonstrated a comparable antitumor effect to DTX solution, the DTX-S-LA/$DSPE_{2K}$ NPs (10 mg/kg) did not cause any weight loss or hepatotoxicity. Safety is an indispensable index in assessing a potential DDS. No material carrier, no Tween 80 made DTX-S-LA/$DSPE_{2K}$ NPs (10 mg/kg) non-toxic and safe. Besides, the tumor burden of DTX-S-LA/$DSPE_{2K}$ NPs (10 mg/kg) was smaller than that of DTX solution. Thus, the low dose nanoassemblies still had certain advantages in the long-term application of anticancer drugs.

Compared with DTX solution, smaller tumor volumes and large necrotic areas could be found in mice treated with DTX-S-LA/$DSPE_{2K}$ NPs (30 mg/kg), indicating the high dose nanoassemblies could effectively inhibit tumor growth and had potent anticancer activity. Notably, the DTX-S-LA/$DSPE_{2K}$ NPs was nontoxic regardless of the dose. On the contrary, the DTX containing Tween 80 solution showed great hepatotoxicity and weight loss in a relatively low dose. This hinted that DTX-S-LA/$DSPE_{2K}$ NPs had a higher maximum tolerated dose than DTX solution so that better anticancer effect could be achieved by increasing dose.

5. Conclusions

In this study, a novel prodrug had been designed and synthetized. The notable advantages of nanoparticles can be concluded as follows. (1) The preparation process is extremely simple and can be scaled up. (2) Avoiding large excipients: the drug loading could rise to 53.4% which is extremely higher than other nanoparticles. (3) LA can be obtained from natural food and it is biodegradable. Furthermore, it can achieve nutrition target drug delivery and against proliferation of cancer. (4) Mono thioether bond is redox dual-responsive which makes the prodrug specific release in tumor. (5) Prolonged circulation time and higher AUC can be achieved. In summary, the redox sensitive prodrug nanoassemblies have the potential capability of resisting cancers and provide unprecedented.

Acknowledgments

This work was supported by Liaoning BaiQianWan Talents Program (No. 2016921064, China) and Nature Science Foundation of Guangdong Province (No. 2016A020217017, China).

Appendix A. Supporting information

Supplementary data associated with this article can be found in the online version at https://doi.org/10.1016/j.apsb.2018.08.008.

References

1. Ehrlichova M, Vaclavikova R, Ojima I, Pepe A, Kuznetsova LV, Chen J, et al. Transport and cytotoxicity of paclitaxel, docetaxel, and novel taxanes in human breast cancer cells. *Naunyn Schmiedebergs Arch Pharmacol* 2005;**372**:95–105.
2. Ye T, Xu W, Shi T, Yang R, Yang X, Wang S, et al. Targeted delivery of docetaxel to the metastatic lymph nodes: a comparison study between nanoliposomes and activated carbon nanoparticles. *Asian J Pharm Sci* 2015;**10**:64–72.
3. Zhang H, Wang K, Zhang P, He W, Song A, Luan Y. Redox-sensitive micelles assembled from amphiphilic mPEG-PCL-SS-DTX conjugates for the delivery of docetaxel. *Colloids Surf B Biointerfaces* 2016;**142**:89–97.

4. Chu C, Xu P, Zhao H, Chen Q, Chen D, Hu H, et al. Effect of surface ligand density on cytotoxicity and pharmacokinetic profile of docetaxel loaded liposomes. *Asian J Pharm Sci* 2016;**11**:655–61.
5. Kim SB, Kok YT, Thuan TV, Chao TY, Shen ZZ. Safety results of docetaxel-(taxotere(*R*))-based chemotherapy in early breast cancer patients of Asia-Pacific region: Asia-Pacific breast initiative II. *J Breast Cancer* 2015;**18**:356–64.
6. Seguin C, Kovacevich N, Voutsadakis IA. Docetaxel-associated myalgia-arthralgia syndrome in patients with breast cancer. *Breast Cancer* 2017;**9**:39–44.
7. Logie J, Ganesh AN, Aman AM, Al-Awar RS, Shoichet MS. Preclinical evaluation of taxane-binding peptide-modified polymeric micelles loaded with docetaxel in an orthotopic breast cancer mouse model. *Biomaterials* 2017;**123**:39–47.
8. Baetke SC, Lammers T, Kiessling F. Applications of nanoparticles for diagnosis and therapy of cancer. *Br J Radiol* 2015;**88**:20150207.
9. Minko T, Rodriguez-Rodriguez L, Pozharov V. Nanotechnology approaches for personalized treatment of multidrug resistant cancers. *Adv Drug Deliv Rev* 2013;**65**:1880–95.
10. Seeta Rama Raju G, Benton L, Pavitra E, Yu JS. Multifunctional nanoparticles: recent progress in cancer therapeutics. *Chem Commun (Camb)* 2015;**51**:13248–59.
11. Lin J, Pan Z, Song L, Zhang Y, Li Y, Hou Z, et al. Design and *in vitro* evaluation of self-assembled indometacin prodrug nanoparticles for sustained/controlled release and reduced normal cell toxicity. *Appl Surf Sci* 2017;**425**:674–81.
12. Nel A, Xia T, Madler L, Li N. Toxic potential of materials at the nanolevel. *Science* 2006;**311**:622–7.
13. da Silva Santos S, Igne Ferreira E, Giarolla J. Dendrimer prodrugs. *Molecules* 2016:**21**.
14. Luo C, Sun J, Sun B, He Z. Prodrug-based nanoparticulate drug delivery strategies for cancer therapy. *Trends Pharmacol Sci* 2014;**35**:556–66.
15. Ren G, Jiang M, Xue P, Wang J, Wang Y, Chen B, et al. A unique highly hydrophobic anticancer prodrug self-assembled nanomedicine for cancer therapy. *Nanomedicine* 2016;**12**:2273–82.
16. Ge Y, Ma Y, Li L. The application of prodrug-based nano-drug delivery strategy in cancer combination therapy. *Colloids Surf B Biointerfaces* 2016;**146**:482–9.
17. Chowdhury P, Nagesh PK, Khan S, Hafeez BB, Chauhan SC, Jaggi M, et al. Development of polyvinylpyrrolidone/paclitaxel self-assemblies for breast cancer. *Acta Pharm Sin B* 2018;**8**:602–14.
18. Sun B, Luo C, Cui W, Sun J, He Z. Chemotherapy agent-unsaturated fatty acid prodrugs and prodrug-nanoplatforms for cancer chemotherapy. *J Control Release* 2017;**264**:145–59.
19. Luo C, Sun J, Liu D, Sun B, Miao L, Musetti S, et al. Self-assembled redox dual-responsive prodrug-nanosystem formed by single thioether-bridged paclitaxel-fatty acid conjugate for cancer chemotherapy. *Nano Lett* 2016;**16**:5401–8.
20. Zock PL, Katan MB. Linoleic acid intake and cancer risk: a review and meta-analysis. *Am J Clin Nutr* 1998;**68**:142–53.
21. Bocca C, Bozzo F, Cannito S, Colombatto S, Miglietta A. CLA reduces breast cancer cell growth and invasion through ERα and PI3K/Akt pathways. *Chem Biol Interact* 2010;**183**:187–93.
22. Llor X. The effects of fish oil, olive oil, oleic acid and linoleic acid on colorectal neoplastic processes. *Clin Nutr* 2003;**22**:71–9.
23. Menéndez JA, del Mar Barbacid M, Montero S, Sevilla E, Escrich E, Solanas M, et al. Effect of γ-linolenic acid and oleic acid on paclitaxel cttotoxicity in human breast cells. *Eur J Cancer* 2001;**37**:402–13.
24. Bae WK, Park MS, Lee JH, Hwang JE, Shim HJ, Cho SH, et al. Docetaxel-loaded thermoresponsive conjugated linoleic acid-incorporated poloxamer hydrogel for the suppression of peritoneal metastasis of gastric cancer. *Biomaterials* 2013;**34**:1433–41.
25. Zhong T, Yao X, Zhang S, Guo Y, Duan XC, Ren W, et al. A self-assembling nanomedicine of conjugated linoleic acid–paclitaxel conjugate (CLA–PTX) with higher drug loading and carrier-free characteristic. *Sci Rep* 2016;**6**:36614.
26. Sun B, Luo C, Yu H, Zhang X, Chen Q, Yang W, et al. Disulfide bond-driven oxidation- and reduction-responsive prodrug nanoassemblies for cancer therapy. *Nano Lett* 2018;**18**:3643–50.
27. Xue P, Liu D, Wang J, Zhang N, Zhou J, Li L, et al. Redox-sensitive citronellol-cabazitaxel conjugate: maintained *in vitro* cytotoxicity and self-assembled as multifunctional nanomedicine. *Bioconjug Chem* 2016;**27**:1360–72.
28. Zhang S, Guan J, Sun M, Zhang D, Zhang H, Sun B, et al. Self-delivering prodrug-nanoassemblies fabricated by disulfide bond bridged oleate prodrug of docetaxel for breast cancer therapy. *Drug Deliv* 2017;**24**:1460–9.
29. Wang J, Sun X, Mao W, Sun W, Tang J, Sui M, et al. Tumor redox heterogeneity-responsive prodrug nanocapsules for cancer chemotherapy. *Adv Mater* 2013;**25**:3670–6.
30. Wang Y, Liu D, Zheng Q, Zhao Q, Zhang H, Ma Y, et al. Disulfide bond bridge insertion turns hydrophobic anticancer prodrugs into self-assembled nanomedicines. *Nano Lett* 2014;**14**:5577–83.
31. ten Tije AJ, Verweij J, Loos WJ, Sparreboom A. Pharmacological effects of formulation vehicles. *Clin Pharmacokinet* 2003;**42**:665–85.
32. Hennenfent KL, Govindan R. Novel formulations of taxanes: a review. Old wine in a new bottle?. *Ann Oncol* 2006;**17**:735–49.